The Annual Peak in the SST Anomaly Spectrum

JENS MÖLLER, DIETMAR DOMMENGET, AND VLADIMIR A. SEMENOV*

Leibniz-Institut für Meereswissenschaften, Kiel, Germany

(Manuscript received 3 May 2007, in final form 9 November 2007)

ABSTRACT

The manner in which monthly mean sea surface temperature anomalies (SSTAs) show enhanced variance at the annual period in the extratropics (an annual peak in the variance spectrum) is illustrated by observations and model simulations. A mechanism, related to the reemergence of winter SST anomalies, is proposed to explain the annual peak in SST spectrum. The idea is supported by the analysis of a hierarchy of models, including Intergovernmental Panel on Climate Change model simulations.

The results of the model experiments further suggest that the annual peak is either weak or absent if decadal SST variability is forced by local air–sea interaction. However, if ocean subsurface temperature variability forces decadal SST variability, the annual peak is much stronger. Strong annual peaks may therefore be seen as an indication of ocean-forced decadal SST variability in the extratropics.

1. Introduction

In his pioneering work, Bjerknes (1964) discussed the development and persistence of midlatitudinal sea surface temperature (SST) anomalies (SSTAs) and their influence on the atmosphere. He postulated that SSTA in the North Atlantic from seasonal to interannual time scales may be explained by local forcing of the atmosphere only, while the SSTA on decadal time scales might also depend on ocean dynamics. This is essentially supported by observational (Deser and Blackmon 1993; Kushnir 1994) and modeling studies (Delworth et al. 1993; Delworth 1996).

The passive role of the ocean is also elaborated in the publication of Hasselmann (1976). He establishes the concept of a climate system, which is divided in a fast (atmosphere) and a slow (ocean) part. In this concept, the SSTAs are only a result of the integration of the atmospheric heat fluxes by the ocean mixed layer (ML), which should be an autoregressive process of the first order (AR1 process). The model introduces the atmospheric forcing as the primary cause of low-frequency SST variability, which is still considered to be the main cause for extratropical SST variability (e.g., Frankignoul 1985; Barsugli and Battisti 1998).

More recent studies have shown that most spectra of extratropical SSTA do not quite follow the AR1 process. Hall and Manabe (1997) demonstrated that the SST variability at some locations cannot be explained by an AR1 process, and more recent studies by Dommenget and Latif (2002), Fraedrich et al. (2004), and Dommenget and Latif (2008) pointed out that the large-scale statistics of SST variability are generally inconsistent with an AR1 process. Using numerical models, they showed that either mixed layer depth (MLD) variability or the interaction of the ML with the submixed layer is responsible for this inconsistency. Thus, the deviations in the SST spectra are still not attributed to lateral ocean dynamics, but correspond to a slightly more complex model of local air–sea interaction. The atmospheric forcing still appears to be the driving force of SST variability.

Namias and Born (1970, 1974), and later Alexander and Deser (1995), describe the reemergence effect of wintertime SST anomalies in the following fall and winter. They described this effect as follows: The deep MLD and strong atmospheric forcings during winter allow for the creation of persistent temperature anomalies in the upper ocean, which are isolated during summer by a shallow MLD. The past winter SSTA reemerges in the subsequent winter when the MLD deepens again. The reemergence effect appears in regions with large differences in the MLD between winter and

* Additional affiliation: Oboukhov Institute of Atmospheric Physics (RAS), Moscow, Russia.

Corresponding author address: Dietmar Dommenget, Leibniz-Institut für Meereswissenschaften, Düsternbrooker Weg 20, 24105 Kiel, Germany.
E-mail: ddommenget@ifm-geomar.de

DOI: 10.1175/2007JCLI2025.1

TABLE 1. All model simulations discussed in this study are shown.

Name	Atmosphere	Ocean	Ocean resolution, lon × lat	Length (yr)	Comment
CCCMA	GCM	GCM	192 × 96	340	IPCC preindustrial
CISRO	GCM	GCM	192 × 189	340	IPCC preindustrial
GISS	GCM	GCM	360 × 180	340	IPCC preindustrial
HADLEY	GCM	GCM	288 × 144	340	IPCC preindustrial
IPSL	GCM	GCM	180 × 170	340	IPCC preindustrial
METEO	GCM	GCM	180 × 170	340	IPCC preindustrial
MRI	GCM	GCM	144 × 111	340	IPCC preindustrial
MPI	GCM	GCM	128 × 117	340	IPCC preindustrial
NCAR	GCM	GCM	320 × 395	340	IPCC preindustrial
ECHAM5-MPI-OM	GCM	GCM	120 × 60	2 × 500	Tropics decoupled
ECHAM5-slab	GCM	Slab	96 × 48	300	No ocean dynamics
ECHAM5-OZ	GCM	Slab	96 × 48	800	Multilayer, no ocean dynamics
ECHAM5-OZfix	GCM	Slab	96 × 48	300	Seasonally prescribed mixed layer depth
BB-OZ	Statistical	Slab	1 × 1	10 000	Sensitivity studies

summer, for example, in the North Pacific or North Atlantic (Alexander et al. 2000; Timlin et al. 2002; Bhatt et al. 1998). Moreover, currents have to be relatively weak and temperature anomalies must be coherent over broad areas (Timlin et al. 2002). De Coëtlogon and Frankignoul (2003) find that a simple SST reemergence model has a broad peak in the SST anomaly spectrum at the annual period.

The present study focuses on this annual peak feature in the variance spectrum of SSTA in the extratropics. We will illustrate that long time series of SST have a peak at the annual period in the variance spectrum of SSTA in both the observations and in the atmosphere–ocean general circulation models (AOGCMs) on top of the red-noise spectrum. The association of this annual peak with the reemergence mechanism and subsurface decadal oceanic variability is investigated. A hypothesis will be introduced to explain this anomalous variance at the period of 1 yr, which will be tested using a one-dimensional ocean mixed layer model.

The paper is organized as follows: In the following section a short description of the observational dataset, the models used, and some definitions of statistical parameters are given. The analyses of observed and simulated SST spectra are presented in section 3. A mechanism for the time-scale interaction between low-frequency subsurface oceanic variability and the annual cycle is described in section 4, which is tested in section 5 with the aid of a simple model. In section 6 the effect of the length of the time series on the appearance of the annual peak will be shortly discussed. The results are summarized and discussed in section 7.

2. Data, models, and methods

A description of all data and models used in this study are given below. Table 1 summarizes all of the model simulations used.

a. Data

For the analysis of observations of sea surface temperature the Hadley Centre Sea Ice and SST (HadISST) dataset with a resolution of 1° × 1° is used. This dataset was chosen because of its relatively long period from 1870 to 2003 and its global coverage (Rayner et al. 2003). The dataset was interpolated onto a coarser 3° × 3° grid. Thus, the presentation of the statistical parameters becomes less noisy.

b. Intergovernmental Panel on Climate Change models

Nine state-of-the-art global coupled ocean–atmosphere general circulation models (CGCMs) are used, which were conducted within the framework of the Fourth Assessment Report (AR4) of the Intergovernmental Panel on Climate Change (IPCC; Solomon et al. 2007). We used only preindustrial control simulations, which were long enough to study the multidecadal variability. External forcing factors are not considered in these simulations, so that we can obtain uncontaminated estimates of the internal variability from the model runs. The following are the nine models from the IPPC database: Canadian Centre for Climate Modeling and Analyzing (CCCMA), Canada; Commonwealth Scientific and Industrial Research Organization (CSIRO), Australia; National Aeronautics and Space Administration (NASA) Goddard Institute for Space Studies (GISS), United States; Met Office Hadley Centre (HADLEY), United Kingdom; Institut Pierre Simon Laplace (IPSL), France; Météo-France (METEO), France; Max Planck Institute for Meteorology (MPI), Germany; Meteorological Research Institute (MRI), Japan; and National Center for Atmospheric Research (NCAR), United States. See Table 1 for a summary of the IPCC models used.

All of the models were considered together, each with a 340-yr time series (3060 yr, in total), and all of the models are interpolated SST onto a common coarser 3° × 3° grid, which provides a multimodel estimate of the SST variability.

c. *ECHAM5 with different ocean models*

In addition to the most realistic CGCMs we used a series of CGCMs using the ECHAM5 atmosphere model coupled to different simplified ocean models. The ECHAM5 is a state-of-the-art atmospheric general circulation model that is run at horizontal resolution of T31 (3.75° × 3.75°) with 19 vertical levels (Roeckner et al. 2003).

1) ECHAM5-SLAB

The ECHAM5 is coupled to a simple slab ocean model, which only simulates the heat capacity of the upper 50 m of the ocean. The ECHAM5-slab was integrated over 300 yr.

2) ECHAM5-OZ

In a second simulation, the ECHAM5 model is coupled to a simple one-dimensional ocean mixed layer model OZ, which is similar to the model of Alexander and Penland (1996). The ocean model OZ is represented by 19 vertical layers that are connected through vertical diffusion only. Thus, ocean grid points do not communicate with lateral neighbors. Density depends on temperature and salinity, but density variations are only temperature driven. The salinity profile is fixed to the climatology of Levitus (1982). The ocean is driven at the surface by heat flux and mechanical wind mixing (Niiler and Kraus 1977). The temperature of the lowest layer at a depth of 500 m is restored to the observed climatology. The effects of the time mean ocean currents are included by a so called Q-flux scheme, which ensures a realistic mean state. Changes in ocean currents, however, are not considered. The ECHAM5-OZ model was integrated for 800 yr.

The model produces realistic monthly mean SST standard deviations, including the seasonal differences, and it has a realistic SST spectrum in the mid- and higher latitudes (Dommenget and Latif 2008). The model produces a realistic reemergence of SST anomalies resulting from a realistic seasonal cycle of the MLD and the storage of winter temperature anomalies in deeper layers. Because of missing ocean dynamics the SST variability in the tropics is much weaker than that observed and has unrealistic spatial structures. The model should therefore only be considered for extratropical SST variability.

3) ECHAM5-OZFIX

The ECHAM5-OZ model is also used with a MLD, which is seasonally prescribed. Thus, the effects of wind mixing and anomalous MLD are neglected, but the reemergence mechanism resulting from the seasonal cycle of the MLD is conserved. The ECHAM5-OZfix model was integrated for 300 yr.

4) ECHAM5-MPI-OM

We further analyzed twin experiments with ECHAM5 T31 resolution coupled to the MPI Ocean Model (MPI-OM) ocean GCM to investigate the role of tropical forcing for the extratropical SST variability. In the control experiment both the ocean and atmosphere are fully coupled, and in the second sensitivity experiment the tropical (20°S–20°N) SST in the Indian and Pacific Oceans is held fixed to the control climatological values. Both simulations are 500 yr long. The experiments are discussed in more detail in Semenov and Latif (2006).

d. *A simple one-dimensional statistical atmosphere OZ model*

For sensitivity studies with the OZ model, we also use the simple one-dimensional statistical atmosphere model following Barsugli and Battisti (1998) to generate realistic heat flux anomalies (termed BB-OZ):

$$\gamma_a \frac{d\tilde{T}_a}{dt} = -\lambda_{oa}(\tilde{T}_a - \tilde{T}_o) - \lambda_a \tilde{T}_a + \tilde{F}_a, \qquad (1)$$

where $\tilde{T}_a$ and $\tilde{T}_o$ are the anomalous atmospheric temperature and SST, respectively. The heat capacity of the atmosphere is given by $\gamma_a = 10^7$ J K^{-1} m^{-2}. The coupling parameter was chosen to be similar to that of Barsugli and Battisti (1998), with $\lambda_{oa} = \lambda_{ao} = 25$ W m^{-2} K^{-1} and $\lambda_a = 30$ W m^{-2} K^{-1}. The weather forcing $\tilde{F}_a$ was chosen to be white noise with a standard deviation of $\sigma(\tilde{F}_a) = 50$ W m^{-2} to generate realistic SST anomaly amplitudes. The anomalous heat flux to the ocean model is given by

$$\tilde{F}_o = -\lambda_{ao}(\tilde{T}_o - \tilde{T}_a). \qquad (2)$$

The model allows the generation of realistic SST variability in the extratropics that is comparable to those of the ECHAM5-OZ simulation. For the mean heat flux, wind stress, ocean temperature, and salinity profiles we used those of the ECHAM5-OZ model at 50°N, 30°W. Wind stress anomalies are random white noise with the standard deviation is identical to that of the ECHAM5-OZ simulation. The model is integrated for 10 000 yr at a daily time step.

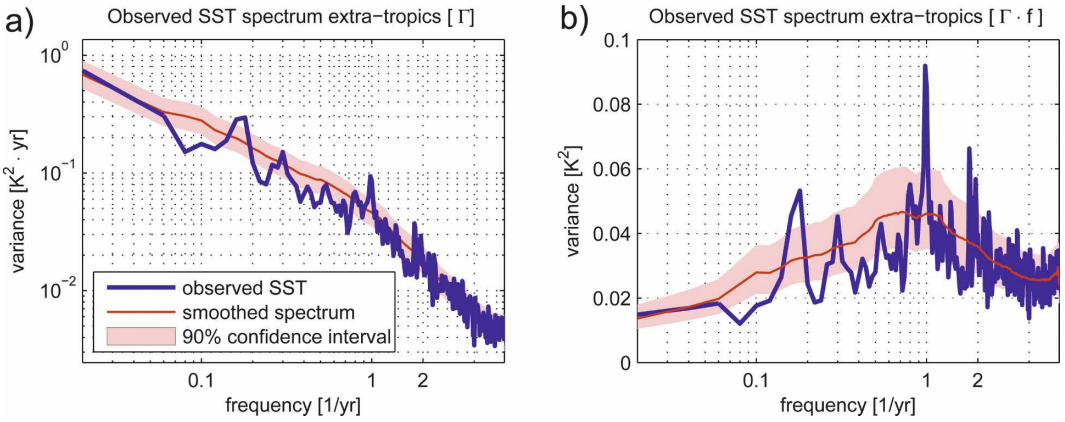

FIG. 1. Observed SST spectrum averaged over ice-free regions from 30° to 55°N: (a) the spectral variance density $\Gamma(f)$, vs frequency in log–log presentation, and (b) $f\Gamma(f)$ over $\log(f)$ in a semilog presentation, which gives a better presentation of the total variance over a $\log(f)$ band. The advantage of the latter representation for mainly red-noise spectra is that peaks on higher frequencies become more visible and the relative importance of these peaks are better represented.

e. Methods

1) ANNUAL VARIANCE RATIO $\mathbf{F}_{1yr}$

The strength of a peak in the variance spectrum can be quantified by comparing the variance at a given frequency band with neighboring frequency intervals. Spectral variance densities are expected to follow a χ^2 distribution, which are usually presented on a logarithmic scaling, because the spread of χ^2-distributed values are proportional to the expected value and are tested on the basis of ratios. We therefore define the annual variance ratio $\mathbf{F}_{1yr}$ as

$$\mathbf{F}_{1yr} = \log(\Gamma_{1yr}) - \frac{1}{2}[\log(\Gamma_{1yr+\delta f}) + \log(\Gamma_{1yr-\delta f})]. \tag{3}$$

Here, $\Gamma_{1yr,\,1yr\pm\delta f}$ is the spectral variance density estimated over a frequency band centered around 1, 1.27, and 0.79 yr^{-1}; $\mathbf{F_{1yr}}$ is defined on the basis of log(10). Thus, values of +1, 0, and −1 refer to a 10, 1, and 0.1 times larger variance Γ_{1yr} relative to the mean of $\Gamma_{1yr+\delta f}$ and $\Gamma_{1yr-\delta f}$.

For a white-noise spectrum the expected value of $\mathbf{F_{1yr}}$ is zero. However, for a red-noise process the expected value is slightly larger than 0, because of the nonlinear spectral slope of the process. For a monthly mean red-noise time series the expected value is smaller than 0.04, depending on the decorrelation time scale of the process.

2) ANNUAL CYCLE AMPLITUDE Υ_{1yr}

The amplitude of the annual cycle for an given year $\Upsilon_{1yr}(t)$ can be defined by projecting the 12-monthly mean SST(m) values of the current year onto the 12-monthly mean values of the normalized mean annual cycle CSST(m) − $\overline{\text{CSST}}$:

$$\Upsilon_{1yr}(t) = \sum_{m=1}^{12} (\text{SST}(m) - \overline{\text{SST}})(\text{CSST}(m) - \overline{\text{CSST}})/12. \tag{4}$$

Here, $\overline{\text{SST}}$ denotes the annual mean of the current year and $\overline{\text{CSST}}$ is the mean over all years; $\Upsilon_{1yr}(t)$ is a temperature value (K). If the mean annual cycle follows a sine function, then $\Upsilon_{1yr}(t)$ is simply the amplitude of the sine function for the current year.

3. Analysis of observed and simulated SST spectra

Figure 1 displays the mean spectrum of observed SSTA (the mean annual cycle is removed), averaged over 30°–55°N. The SST spectrum is mainly a red-noise spectrum, with increased variance toward longer periods. The spectrum shows some fluctuations around the mean red-noise slope at different periods; the strongest deviation from the smoothed spectrum is clearly at the annual period (see Fig. 1b).

Given one mean spectrum, the peak at the annual period may be regarded as a fluctuation. It can, however, be illustrated that peaks at the annual period are a more general feature of monthly mean SST spectra.

Figure 2 displays a global map of the annual variance ratio $\mathbf{F}_{1yr}$ [see Eq. (3) for a definition]. Regions with positive values indicate enhanced variance relative to a linear (log scale) increasing spectrum [for a definition see section 2e(1)]. We can see that most regions, espe-

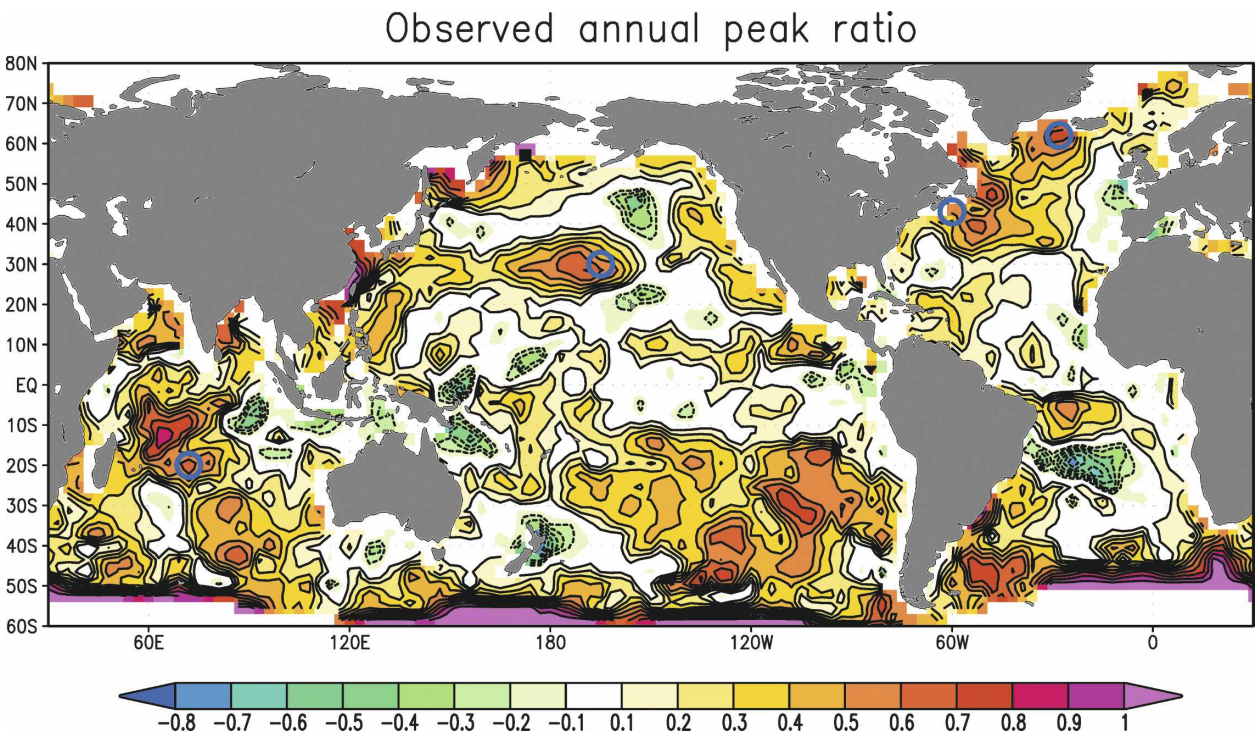

FIG. 2. Global map of the annual peak ratio $\mathbf{F}_{1yr}$ of observed monthly mean SST anomalies. The four marked locations are shown in Fig. 3. Scaling is in logarithmic units; values of +1, 0, and −1 refer to 10, 1, 0.1.

cially at higher latitudes, have an annual peak. In Fig. 3 the spectra at four locations are depicted, which show enhanced variance at the annual cycle. Apparent in both the examples and Fig. 1b is enhanced variance, not only at the annual cycle, but also at the semiannual cycle. The semiannual cycle variance reflects the presence of a semiannual cycle in the mean annual cycle.

We now analyze model simulations, which not only provide longer time series of "perfect" (but model dependent) SST data and give more robust estimates of the statistical parameters, but also enable the discussion of possible physical processes associated with the annual peak by comparing models with different complexities in the simulation of ocean processes.

Figure 4a shows the mean spectrum of midlatitude SST anomalies in the IPCC model ensemble. Because of the much longer time series we can now clearly see the annual and semiannual peak in the SST anomaly spectrum. Note that this feature is present in eight of the nine IPCC models, with larger peaks than the IPCC model ensemble (Fig. 4a) for GISS, METEO, MPI, CCCMA, smaller peaks for IPSL and CSIRO. The HADLEY and NCAR simulations show just about the same amplitudes and the MRI model shows no indication of peaks in the spectrum at any period (not shown).

Figures 4b–d show the analogous spectrum for the CGCMs with the simplified ocean models. The ECHAM5-OZ and ECHAM-OZfix models show some weak indication of an annual and semiannual peak, but they are much weaker than the fully dynamical IPCC models. The ECHAM5-slab model essentially represents the Hasselmann (1976) null hypothesis for SST variability (red noise), which shows no annual or semiannual peaks. The differences between the models indicate that the annual peak may be related to the seasonally varying mixed layer depth and the associated reemergence mechanism, the process by which the ECHAM-OZfix model deviates from ECHAM5-slab. It further seems that ocean dynamics (cf. IPCC models with ECHAM5-OZ) amplify the annual peak characteristics considerably.

Tropical SST variability is a possible forcing for extratropical SST that is not simulated in the ECHAM5-OZ simulation, which may influence the annual peak. We analyzed twin experiments with the ECHAM5-MPI-OM to investigate the role of tropical forcing (see Fig. 5). We can see that the SST spectrum of extratropical SST in the control simulation has a strong peak at about a 4-yr period, indicating the response to tropical Pacific El Niño variability. In comparison to the experiment with the tropical SST variability removed, we can see that the interannual-to-decadal variability is re-

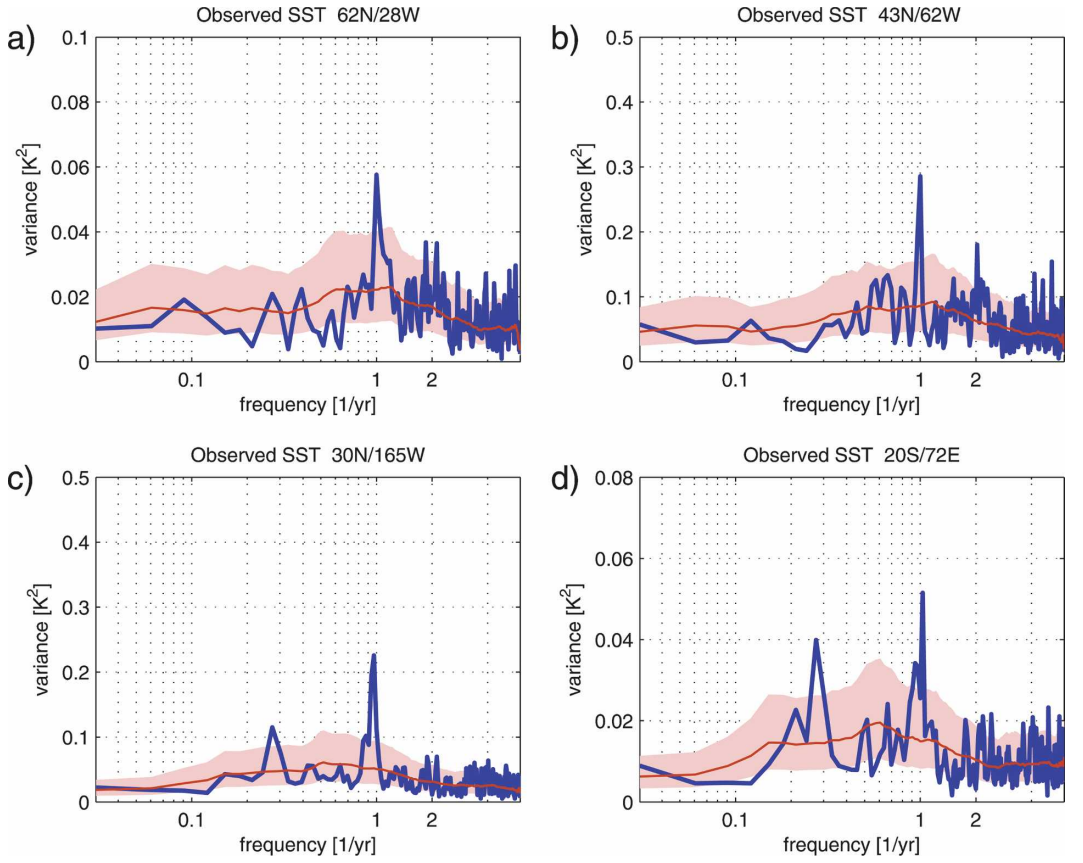

FIG. 3. Observed SST spectrum at four locations, marked in Fig. 2.

duced by about 10%–20%, but the annual peak is essentially unaffected. The annual peak is even more pronounced when tropical SST variability is absent. From this experiment we conclude that the annual peak is essentially independent of tropical forcing.

Figure 6 displays the map of the annual peak ratio $\mathbf{F}_{1yr}$ for the IPCC models ensemble. The map shows that enhanced annual variance is predominantly present at higher latitudes, but is mostly absent in the tropics. The IPCC models show much weaker annual peaks in lower latitudes compared to the observations, especially in the tropical Indian Ocean. Some deviations may arise from the global warming trend in the observations, which are not included in the models. However, one has to be careful in the interpretation of the observational annual peaks, which are much more uncertain than the models, because of the reduced data quality of the seasonal cycle over most regions and the much shorter time series.

We can compare the observations with different models by zonally averaging the annual peak ratio $\mathbf{F}_{1yr}$ (see Fig. 7). The observations and the IPCC models show good agreement with the tendency for the annual peak to be stronger at higher latitudes. The ECHAM5-slab model essentially fluctuates around zero, indicating no annual peak and the ECHAM5-OZ and ECHAM5-OZfix models show a latitude-independent, spatially uniform, and weak annual peak of similar strengths, with some enhancement near the western boundaries.

4. A mechanism for the interaction between decadal variability and the annual cycle

The annual peak in SST anomaly spectra reflects an annual cycle in SST anomalies, which appears to be related to the seasonal cycle of the MLD, as indicated by the comparison of the different simple ocean models coupled the ECHAM5 atmosphere model. A similar characteristic, of a combination of an annual cycle in SST anomalies and the annual cycle of the MLD, has been discussed in the context of reemergence of SST anomalies in the extratropics (Alexander and Deser 1995). The reemergence mechanism is the basis for understanding the annual peak in SST anomaly spectra. De Coëtlogon and Frankignoul (2003) showed that a

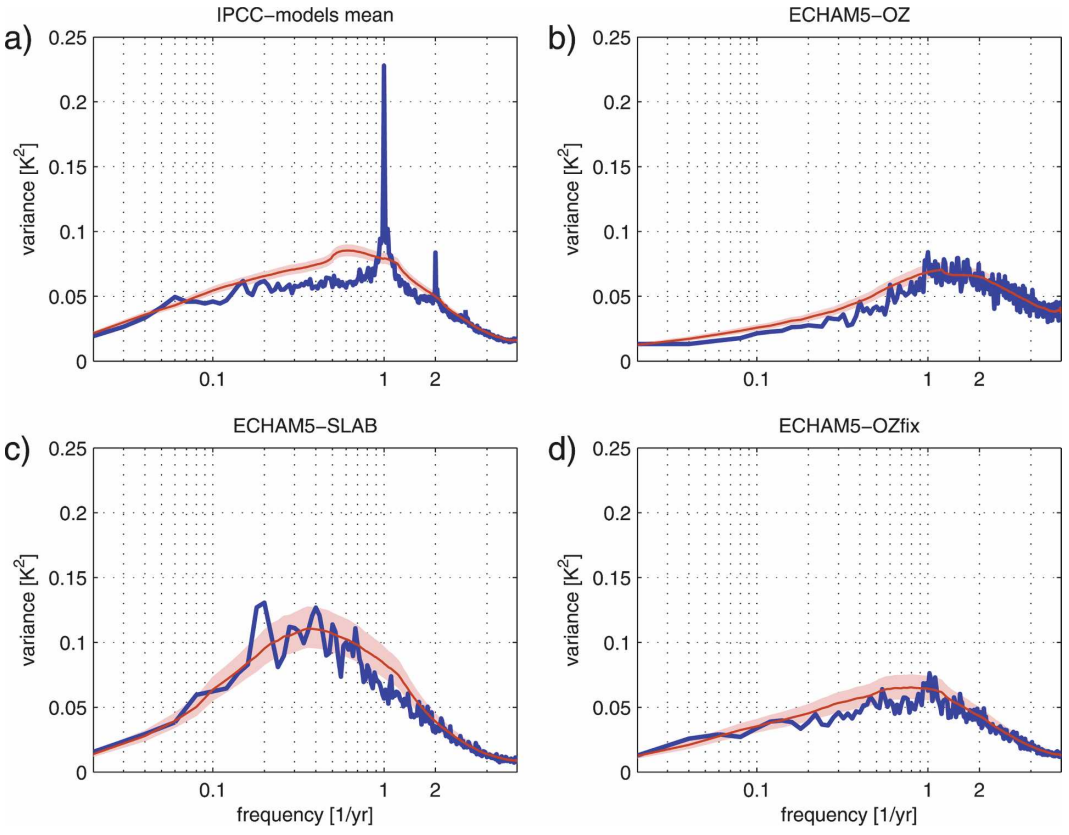

FIG. 4. As Fig. 1, but for different model simulations.

simple conceptual model that includes the reemergence mechanism has a broad peak in the SST anomaly spectrum at the annual period.

Figure 8a displays a section from a time series of the SST and temperatures at 250-m depth (T_{250m}) of the IPCC-GISS model in the North Atlantic to illustrate this mechanism. This depth of 250 m is approximately below the mean wintertime MLD. The time series shows that the SST during winter follows the variations of T_{250m} quite well. During the summer the SST does not follow the variations of T_{250m} as well, with the mean deviations from the mean annual cycle somewhat smaller than in wintertime (e.g., year 270, 285, and 289). This type of behavior is found in most IPCC models, but not in those with smaller or no annual peaks (IPSL, MRI, and CSIRO).

In Fig. 8b the mechanism for the time-scale interaction is displayed more clearly with the aid of a simplified sketch. For this sketch we added a decadal subsurface temperature variability (blue line) to a seasonal cycle SST (black line), but scaled the amplitude with a seasonal scaling factor. The decadal signal is fully present only in wintertime and fully absent during summertime (red line). The resulting SST anomaly time series (green line) has a decadal signal and an anomalous seasonal cycle during the peak phases of the decadal signal. Thus, the seasonal cycle of the SST anomalies is modulated by the decadal variability. Subsequently, the spectra of SST anomalies will show not

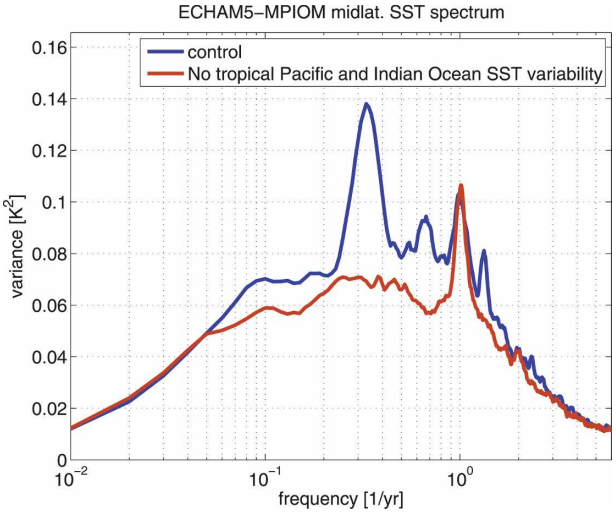

FIG. 5. As Fig. 1, but for the ECHAM5-MPI-OM simulations.

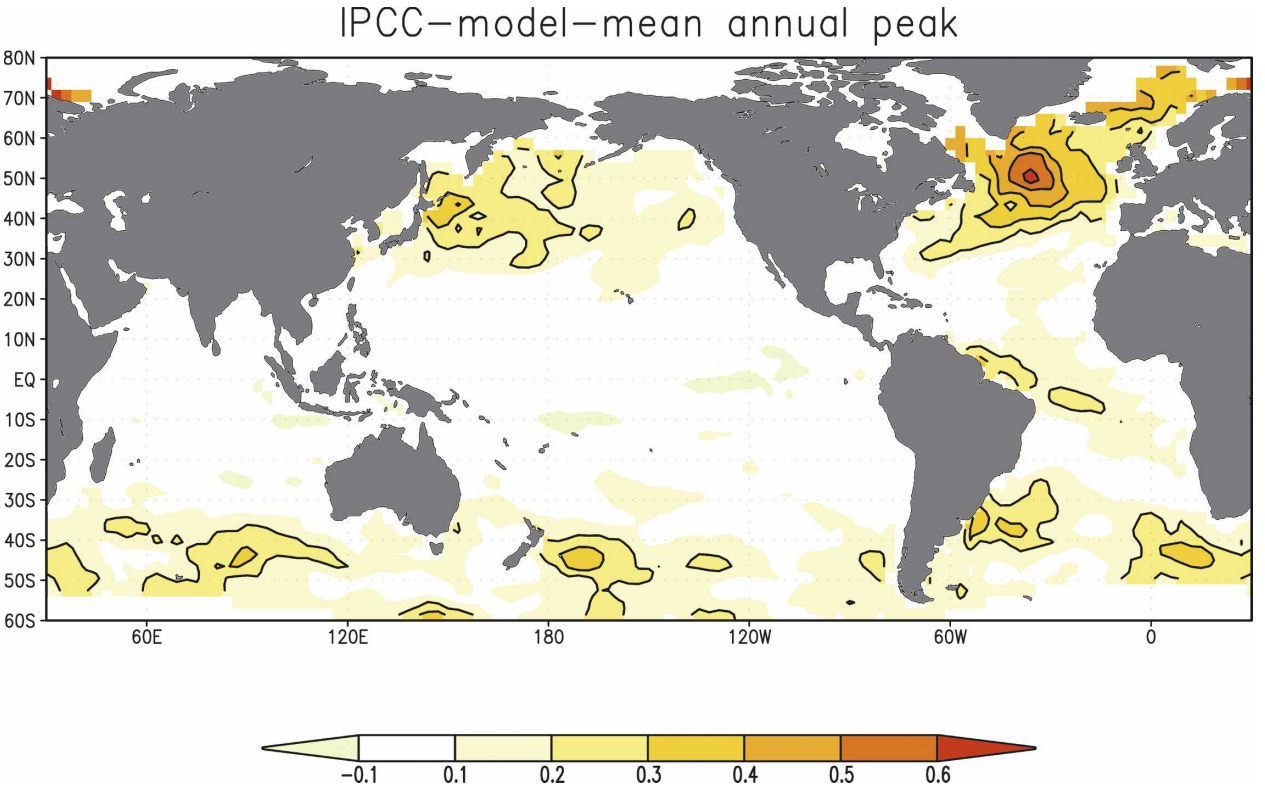

FIG. 6. Global map of the annual peak ratio $\mathbf{F}_{1yr}$ as in Fig. 2, but for the mean of all IPCC models.

only large decadal variance, but also a peak at the annual frequency.

Further, this mechanism indicates that the strength of the annual cycle is correlated to the decadal anomaly. A positive (negative) decadal temperature anomaly, which appears only during winter, reduces (enhances) the annual cycle of this year, which suggests an anticorrelation between the decadal SST anomalies and the strength of the annual cycle. If anomalies appear only during summertime we would find a positive correlation between the annual mean and the annual cycle amplitude. A similar mechanism, but on a shorter time scale, has been described by Gu and Philander (1995) for the interaction of El Niño with the annual cycle of the tropical Pacific SST.

The above relation between the annual mean and the annual cycle amplitude variability can be quantified by a cross-spectral analysis between the annual mean SST and a time series of the strength of the annual cycle Υ_{1yr} [see Eq. (4) for a definition], which is shown in Fig. 9 for the mean of all of the IPCC models averaged over the midlatitudes. The spectral variance of Υ_{1yr} is smaller than that of the SST, but has a similar red-noise behavior, with the largest variance at multidecadal time scales. The covariance is therefore also strongest at the decadal-to-multidecadal time scales.

The coherence between the annual mean and annual cycle variance is generally around 0.3, but it is increased on the shortest periods of year-to-year variability. The phase relation on the shorter time scales is in phase, which corresponds to a positive correlation on the year-

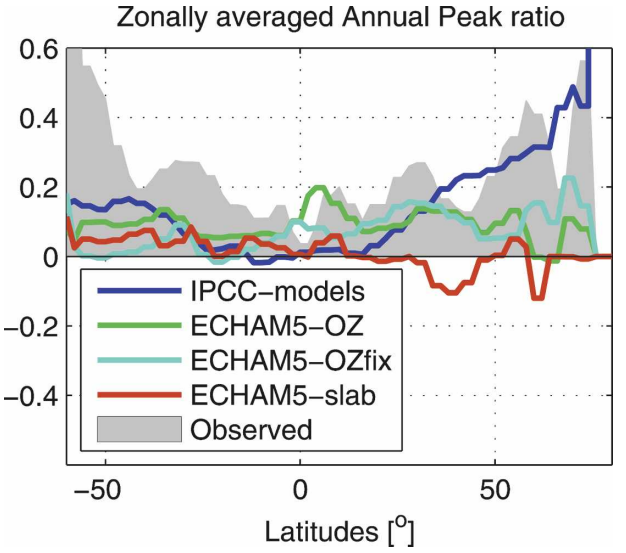

FIG. 7. Zonal mean annual peak ratio $\mathbf{F}_{1yr}$ of observed and simulated monthly mean SST.

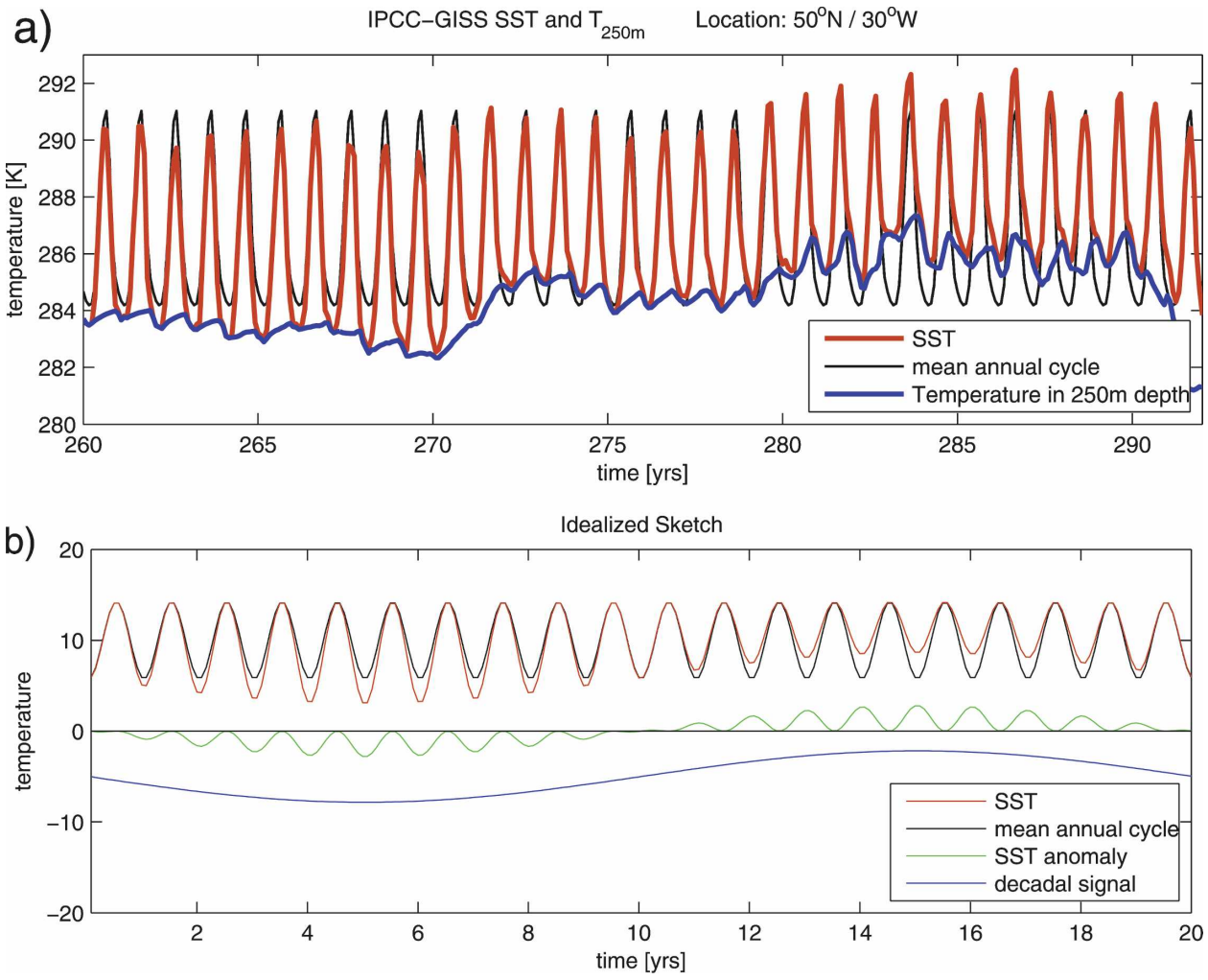

FIG. 8. (a) A section of the SST and 250-m-depth ocean temperature (blue line) time series of the IPCC model GISS, and (b) an idealized sketch of SST variability.

to-year basis. On longer time scales the phase relation shifts to 180°, which refers to a negative correlation on these time scales. This phase relation on longer time scales is consistent with the discussion of Fig. 8. The reemergence mechanism further suggest that the coherence between the annual cycle and the subsurface temperatures should be even larger. This can be estimated by the cross spectrum between the February–March SST and Υ_{1yr}, which is about 0.45 for decadal and longer periods (not shown), thus supporting the reemergence mechanism.

The positive correlation on short time scales indicates that the annual mean variation on this time scale is dominated by summertime variability. This seems to be plausible, because summertime variability is much stronger on seasonal time scales than wintertime variability.

The reemergence mechanism (Alexander and Deser 1995; de Coëtlogon and Frankignoul 2003) describes the wintertime SST anomalies as being generated by atmospheric forcing, which can be simulated in a simple vertical mixed layer model, such as the ECHAM5-OZ model. The ECHAM5-OZ model indeed simulates the features describe by Alexander and Deser (1995) and de Coëtlogon and Frankignoul (2003), but does not simulate the strong annual peak as observed or simulated in the IPCC models (see Figs. 4 and 7). This suggests that the dynamical ocean models have another process that is important for the annual peak.

A signature of the IPCC models that may be relevant for the annual peak is a generally larger temperature variability below the base of the wintertime MLD, compared to the ECHAM5-OZ model. In the ECHAM5-OZ simulation, temperature variability is entirely gen-

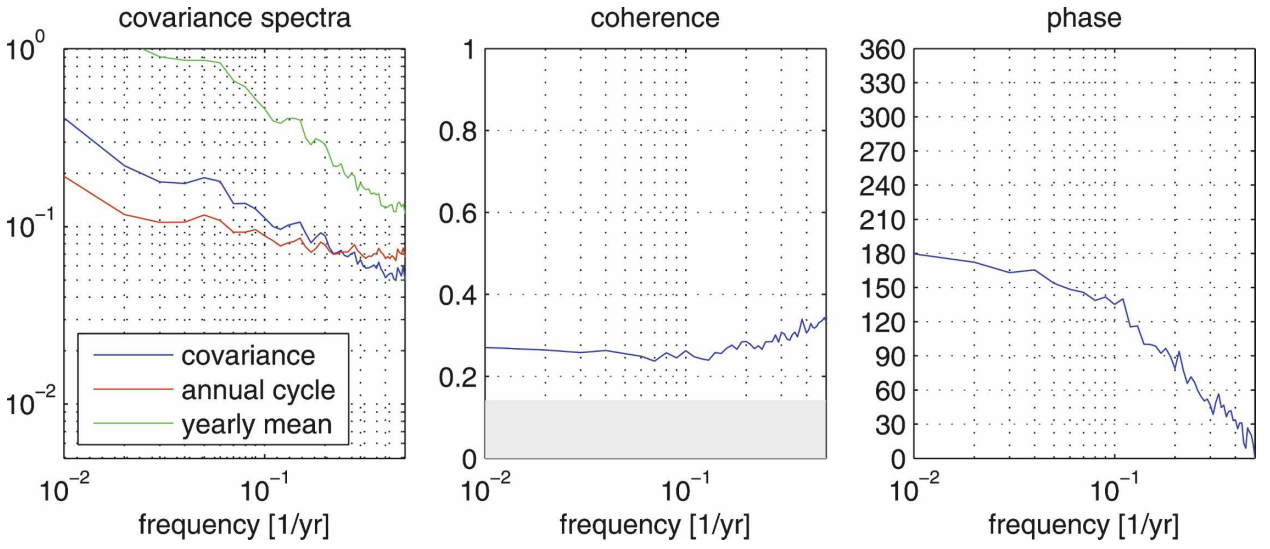

FIG. 9. Mean of all IPCC model cross-spectral analysis between the annual mean SST and the annual cycle amplitude Υ_{1yr} over ice-free regions from 30° to 55°N. The gray area in the coherence panel indicates the 99% confidence interval for zero coherence.

erated by atmospheric forcing and is therefore forced from the surface to the deeper layers. The standard deviation of the temperature thus decreases monotonically with depth (not shown). In the IPCC models most extratropical regions have at least equally strong temperature variability at the surface and below the base of the wintertime MLD. In some locations were the annual peak is relatively strong we found that the temperature variability below the base of the wintertime MLD is even stronger than the SST variability. This increased deep temperature variability in the IPCC models, compared to the simple ECHAM5-OZ model, indicates that the annual peak in large part may be a reflection of the interaction of the local ML dynamics and the internal oceanic variability.

5. Sensitivity studies with a one-dimensional mixed layer model

The concept of the reemergence mechanism suggests that the ECHAM5-OZ model should in principle be able to produce the annual peak in the spectrum of SST anomalies, if the ocean subsurface temperature or wintertime SST anomalies are strong enough, which does not seem to be the case in the ECHAM5-OZ simulation. We therefore conducted sensitivity studies with the simple statistical atmosphere model of Barsugli and Battisti (1998) coupled to the one-dimensional ocean mixed layer model (BB-OZ; see section 2d for details on the model). Note that the BB-OZ model is essentially the stochastic climate model of Hasselmann (1976), extended by a seasonal cycle of the mixed layer and the associated reemergence and feedback to the atmosphere.

We conducted one control experiment and two experiments in which we artificially introduced decadal temperature anomalies. In both sensitivity experiments we introduced a red-noise time series with a decorrelation time scale of about 10 yr. In the first experiment we introduced the time series into the subsurface ocean layers (at around 200-m depth), with a weak Newtonian adjustment (a coupling time scale of about 2 yr). In the second experiment we introduced the time series into the atmospheric temperature T_a with a Newtonian adjustment of $\lambda = 25$ W m^{-2} K^{-1}. Because of the Newtonian approach, the standard deviation in both simulations was adjusted to produce the effective standard deviation of the signal of about 1.0 K in the subsurface ocean layer and at the atmospheric temperature T_a. Each simulation and a control simulation was integrated over 10^4 yr.

Figure 10 shows the spectra of the sensitivity experiments in comparison to a control experiment. Note that the control simulation of BB-OZ shows the annual peak, which is in agreement with the much simpler conceptual model of de Coëtlogon and Frankignoul (2003). The strength of this annual peak in the BB-OZ model depends on the seasonal cycle of the MLD, the heat fluxes ($\tilde{F}_a$), and the wind stress. Strong seasonal cycles in each of these quantities favor the existence of the annual peak.

If a decadal signal is put into the subsurface ocean temperature, the SST anomaly spectrum shows a strong annual peak. However, an equally strong signal forced

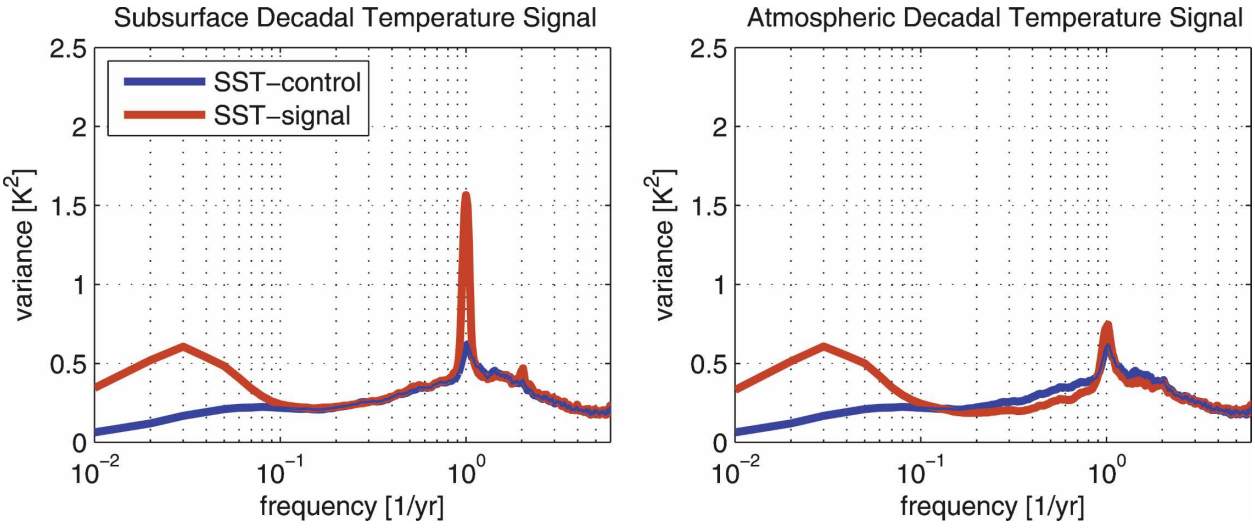

FIG. 10. Spectra of SST anomalies from the simple one-dimensional atmosphere OZ model sensitivity runs.

from the atmospheric temperatures does not produce an equally strong annual peak. These sensitivity studies therefore suggest that the annual peak in the observed SST and in the IPCC models' SST may be understood in the context of the mixed layer ocean model if additional subsurface ocean temperature variability is introduced.

The sensitivity experiments can be repeated with the OZfix model, using the seasonally prescribed MLD. The results are essentially the same, but the OZ model with interactive MLD is more sensitive to temperature anomalies below the mean wintertime MLD, leading to stronger decadal SST anomalies and to slightly stronger annual peaks. However, these results depend on the MLD climatology and on the position of the subsurface ocean temperature anomalies.

6. Effects of the length of the time series

The expected value of the variance density of a power spectrum $\Gamma(f)$ usually is not dependent on the length of the time series. The length of the time series generally only effects the uncertainty of $\Gamma(f)$. However, the annual peak value caused by the decadal modulation of the annual cycle of SST will be affected by the length of the time series, because the estimation of the mean annual cycle is done over the same limited time series.

To illustrate the impact of the length of the time series onto the annual peak value, we calculated the variance spectrum of the SST anomalies in the sensitivity run in section 5 of Fig. 10a based on time series with different lengths (see Fig. 11). Note that the simple model is used only to have long statistics, but the results are equally valid for the IPCC models; however, the observations are too short to illustrate this effect.

The spectrum Γ_{long} is based on a 10^4-yr-long time series with the mean annual cycle of the entire period removed (identical to the red line in Fig. 10a). The spectrum Γ_{short} is the mean of 250 $\times$ 40 yr long time series, with the mean annual cycle of only the corresponding 40-yr time period removed for each of 250 time series. Thus, Γ_{short} represents the spectrum of a time series for which only 40 yr of data are available.

The comparison of Γ_{long} and Γ_{short} shows that the

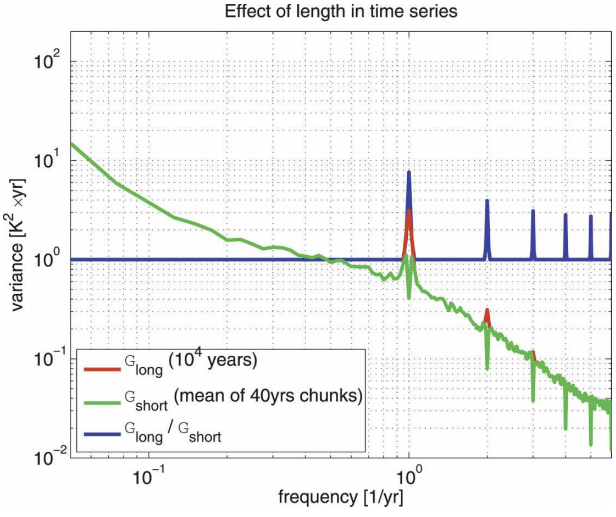

FIG. 11. Spectrum of SST anomalies from the sensitivity simulation as in Fig. 10a estimated from long and short time series. Anomalies are defined for the long and short time series individually, by subtracting the mean annual cycle of the corresponding time series.

spectral variance density is the same for both estimates at all frequencies except for the annual frequency and its subharmonics. The reduced variance at annual frequency and its subharmonics are caused by subtracting the mean annual cycle of the relatively short time period and therefore subtracting a significant fraction of the anomalous decadal modulation of the annual cycle. Most observational datasets of SST are much shorter than the HADISST dataset, and the annual peak will, therefore, not be detectable within these shorter time series.

7. Summary and discussion

In this study we have analyzed the observed spectrum of monthly mean SST anomalies of 100-yr-long time series. The spectrum shows a weak indication of a peak at the annual frequency, which appears to be a global feature, with the strongest amplitudes at high latitudes.

To better understand this signature we have analyzed a series of model simulations with much longer statistics and varying complexity in the representation of the ocean processes. The IPCC model simulations clearly illustrate that the annual peak is a significant feature of monthly mean SST anomaly spectra, which have a clear dependence on the latitudes. The annual peak amplitude is small in the tropics and increases with latitude. The signature of the annual peak is missing in coupled simulations with a simple slab ocean model, which simulates neither the annual cycle of the MLD nor the reemergence process. A simple local one-dimensional mixed layer model (OZ) that can simulate the seasonal cycle of the MLD and the reemergence process does show some indications of the annual peak being similar to the simple conceptual model of de Coëtlogon and Frankignoul (2003), but the signature is much weaker compared to the fully dynamical ocean models. However, the annual peak can be simulated in the OZ model if additional subsurface decadal ocean temperature variability is introduced. We therefore conclude that the annual peak is a reflection of the reemergence mechanism. Decadal SST anomalies are more pronounced in wintertime, which lead to a seasonal cycle of SST anomalies. This annual cycle of the SST anomalies manifests itself in an annual peak in the variance spectrum. This mechanism leads to a weak covariance of the annual mean SST and the strength of the annual cycle in the IPCC models. The strength of the annual cycle is slightly anticorrelated to the decadal SST variability.

We think that the main difference between the fully dynamical ocean models and the simple local mixed layer ocean model is that the fully dynamical ocean models additionally can generate temperature, or, more generally, density variations in the subsurface ocean that are essentially independent of local atmosphere forcing or are at least mainly forced from ocean internal processes. This oceanic variability is picked up by the deep wintertime mixed layer and brought to the surface, leading to the stronger annual peak in the SST spectrum. A simple coupled GCM experiment by Cassou et al. (2007) showed that subsurface temperature anomalies introduced into the submixed layer of the North Atlantic do indeed reemerge in the subsequent fall and winter and influence the SST and atmosphere.

On the other hand, if the local ocean model ECHAM5-OZ integrates atmospheric forcings, even those including strong decadal signals, the annual peak signature in the SST spectrum is much weaker. Thus, it appears that the annual peak signature is more efficiently forced by oceanic variability. This in turn means that, in regions with strong annual peaks, the covariance between the time series of multidecadal variability of the annual cycle strength Υ_{1yr} and the annual mean time series is covariant with ocean-forced decadal variability. The atmospheric-forced decadal variability will have a weak covariance in these regions. Because subsurface ocean data are rarely observed over long time periods (many decades), time series of Υ_{1yr} could be a first-guess proxy for the subsurface ocean temperature variability on multidecadal time scales in regions with strong annual peaks.

The causes of nonlocal subsurface ocean variability can be different at different regions and may be a complex interaction between atmospheric forcings and the upper ocean currents and stratification. The regional structure of the annual peak strength in the IPCC models suggests that the kind of variability that may cause the annual peak is increasing with latitude and has pronounced strength in the west North Pacific, where the Kuroshio leaves the coast, near the Bering Sea, and in the central-northern North Atlantic. The main nonlocal processes that are not simulated in the ECHAM5-OZ simulations are Ekman pumping resulting from large-scale wind curls, Rossby waves, and ocean current variability, such as mesoscale eddies or meandering of currents. Both Ekman pumping and Rossby waves can affect the thermocline depth and therefore cause SST variability. Both are also consistent with the increase of variability with latitude. Miller and Schneider (2000) pointed out that the SST variability near the Bering Sea, a region with a relatively strong annual peak, is caused by Ekman pumping resulting from the large-scale wind curl of the Aleutian low and the SST variability in the west North Pacific, where the Kuroshio leaves the coast, that are related to Rossby waves. This

is again a region with a relatively strong annual peak. They further find that local processes are more important in the central North Pacific, which seems to be consistent with the weaker annual peak amplitude in this region.

It may further be noted that tropical SST variability is a significant forcing of the extratropical SST, which may amplify the decadal SST variability in the extratropics. Here it may be of particular interest, because the tropical Pacific SST variability has a pronounced seasonal cycle, which in the real world may affect the annual peak mechanism, but did not in our ECHAM5-MIP-OM model.

However, we have to note that the mechanism proposed in this study is based on model results, while the observational records could neither support nor reject this mechanism. Much of the conclusions drawn are dependent on the ability of the ECHAM5-OZ model to simulate the mechanism. It would therefore be helpful to verify the results with other models or a better spatial resolution. We think that the observational record is currently too short and too limited in quality to analyze the details of the annual peak phenomenon (e.g., cross-spectral analysis is too noisy). One quality limitation in the HADISST dataset may be the limited number of observations per year and per grid point over the early decades of the dataset. However, detailed analysis of high-quality profiles in regions with many decades of seasonally resolved data may help to study the phenomenon.

Another aspect that is currently not well understood, which is not discussed in this analysis, is the effect of subsurface salinity variability, which in many cases is coherent with subsurface temperature variability. While the salinity has no direct effect on the SST, it will have an effect onto the MLD and its seasonal cycle. It is therefore likely that subsurface salinity variability may also have an effect on the annual peak of SST anomaly spectra. For example, larger salinity in the subsurface could stabilize the summer ML, which would lead to reduced ML deepening during the early fall season. Such a mechanism would cause warm SST anomalies in the late summer to early fall. The same salinity anomaly could result into cold SST anomalies during the winter season, depending on the mean temperature profiles and the atmospheric forcing. Subsequently, the subsurface salinity anomaly could cause annual cycle variations, while the annual mean SST is undisturbed. The combined effect of temperature and salinity variability in the subsurface may therefore lead to variability that could be understood in terms of annual mean variability and annual cycle variability.

Acknowledgments. We like to thank Carsten Eden and Karina Affler for helpful comments and proofreading. Comments of the editor Shang-Ping Xie and the three reviewers helped to improve the presentation of this paper significantly. The work was supported by the Deutsche Forschungsgesellschaft Sonderforschungsbereich 460. We acknowledge the modeling groups for making their model output available as part of the WCRP's CMIP3 multimodel dataset, the Program for Climate Model Diagnosis and Intercomparison (PCMDI) for collecting and archiving this data, and the WCRP's Working Group on Coupled Modeling (WGCM) for organizing the model data analysis activity. The WCRP CMIP3 multimodel dataset is supported by the Office of Science, U.S. Department of Energy.

REFERENCES

Alexander, M. A., and C. Deser, 1995: A mechanism for the recurrence of wintertime midlatitude SST anomalies. *J. Phys. Oceanogr.,* **25,** 122–137.

——, and C. Penland, 1996: Variability in a mixed layer ocean model driven by stochastic atmospheric forcing. *J. Climate,* **9,** 2424–2442.

——, J. D. Scott, and C. Deser, 2000: Processes that influence sea surface temperature and mixed layer depth in a coupled model. *J. Geophys. Res.,* **105,** 16 823–16 841.

Barsugli, J. J., and D. S. Battisti, 1998: The basic effects of atmosphere–ocean thermal coupling on midlatitude variability. *J. Atmos. Sci.,* **55,** 477–493.

Bhatt, U. S., M. A. Alexander, D. S. Battisti, D. D. Houghton, and L. M. Keller, 1998: Role of atmosphere–ocean interaction in North Atlantic climate variability. *J. Climate,* **11,** 1615–1632.

Bjerknes, J., 1964: Atlantic air-sea interaction. *Advances in Geophysics,* Vol. 10, Academic Press, 1–82.

Cassou, C., C. Deser, and M. A. Alexander, 2007: Investigating the impact of reemerging sea surface temperature anomalies on the winter atmospheric circulation over the North Atlantic. *J. Climate,* **20,** 3510–3526.

de Coëtlogon, G., and C. Frankignoul, 2003: The persistence of winter sea surface temperature in the North Atlantic.. *J. Climate,* **16,** 1364–1377.

Delworth, T. J., 1996: North Atlantic interannual variability in a coupled ocean–atmosphere model. *J. Climate,* **9,** 2356–2375.

——, S. Manabe, and R. J. Stouffer, 1993: Interdecadal variations of the thermohaline circulation in a coupled ocean–atmosphere model. *J. Climate,* **6,** 1993–2011.

Deser, C., and M. L. Blackmon, 1993: Surface climate variations over the North Atlantic Ocean during winter: 1900–1989. *J. Climate,* **6,** 1743–1753.

Dommenget, D., and M. Latif, 2002: Analysis of observed and simulated SST spectra in the midlatitudes. *Climate Dyn.,* **19,** 277–288.

——, and ——, 2008: Generation of hyper climate modes. *Geophys. Res. Lett.*, **35,** L02706, doi:10.1029/2007GL031087.

Fraedrich, K., U. Luksch, and R. Blender, 2004: 1/f model for long-time memory of the ocean surface temperature. *Phys. Rev. E,* **70,** doi:10.1103/PhysRevE.70.037301.

Frankignoul, C., 1985: Sea surface temperature anomalies, planetary waves and air-sea feedback in the middle latitudes. *Rev. Geophys.,* **23,** 357–390.

Gu, D., and S. G. H. Philander, 1995: Secular changes in annual and interannual variability in the tropics during the past century. *J. Climate,* **8,** 864–876.

Hall, A., and S. Manabe, 1997: Can local linear stochastic theory explain sea surface temperature and salinity variability? *Climate Dyn.,* **13,** 167–180.

Hasselmann, K., 1976: Stochastic climate models. Part I: Theory. *Tellus,* **28,** 473–485.

Kushnir, Y., 1994: Interdecadal variations in North Atlantic surface temperature and associated atmospheric conditions. *J. Climate,* **7,** 141–157.

Levitus, S., 1982: *Climatological Atlas of the World Ocean*. NOAA Prof. Paper 13, 173 pp. and 17 microfiche.

Miller, A. J., and N. Schneider, 2000: Interdecadal climate regime dynamics in the North Pacific Ocean: Theories, observations and ecosystem impacts. *Prog. Oceanogr.,* **47,** 355–379.

Namias, J., and R. M. Born, 1970: Temporal coherence in North Pacific sea-surface temperature patterns. *J. Geophys. Res.,* **75,** 5952–5955.

——, and ——, 1974: Further studies of temporal coherence in North Pacific sea surface temperatures. *J. Geophys. Res.,* **79,** 797–798.

Niiler, P. P., and E. B. Kraus, 1977: One-dimensional models of the upper ocean. *Modelling and Prediction of the Upper Layers of the Ocean,* E. B. Kraus, Ed., Pergamon Press, 143–172.

Rayner, N. A., D. E. Parker, E. B. Horton, C. K. Folland, L. V. Alexander, D. Rowell, E. C. Kent, and A. Kaplan, 2003: Global analyses of sea surface temperature, sea ice, and night marine air temperature since the late nineteenth century. *J. Geophys. Res.,* **108,** 4407, doi:10.1029/2002JD002670.

Roeckner, E., and Coauthors, 2003: The atmospheric general circulation model ECHAM5. Part I: Model description. Max Planck Institute for Meteorology Rep. 349, 127 pp.

Semenov, V., and M. Latif, 2006: Impact of tropical Pacific variability on the mean North Atlantic thermohaline circulation. *Geophys. Res. Lett.,* **33,** L16708, doi:10.1029/2006GL026237.

Solomon, S., D. Qin, M. Manning, M. Marquis, K. Averyt, M. M. B. Tignor, H. L. Miller Jr., and Z. Chen, Eds. 2007: *Climate Change 2007: The Physical Sciences Basis.* Cambridge University Press, 996 pp.

Timlin, M. S., M. A. Alexander, and C. Deser, 2002: On the reemergence of North Atlantic SST anomalies. *J. Climate,* **15,** 2707–2712.